Proteolytic Cleavage of the Developmentally Important Cadherin BT-R_1 in the Midgut Epithelium of *Manduca sexta*†

Mehmet Candas,‡,§ Brian R. Francis,§,|| Natalya B. Griko,‡,§ Eric G. Midboe,‡ and Lee A. Bulla, Jr.*,‡

Center for Biotechnology and Bioinformatics and Department of Molecular and Cell Biology, The University of Texas at Dallas, Richardson, Texas 75083, and Department of Molecular Biology, University of Wyoming, Laramie, Wyoming 82071

Received June 18, 2002; Revised Manuscript Received August 9, 2002

ABSTRACT: BT-R_1 (M_r = 210 kDa) represents a new type of insect cadherin that is expressed specifically in the midgut epithelium during growth and development of *Manduca sexta* larvae. It also is a target receptor for the Cry1A toxins of the entomopathogenic bacterium *Bacillus thuringiensis*. Expression of BT-R_1, which varies during larval development, correlates with the abundance of the protein and with the differential cleavage of the molecule at each developmental stage. The cleavage of BT-R_1 is calcium dependent, and consequently, Ca^{2+} directly influences the structural integrity of BT-R_1. Indeed, removal of calcium ions by chelating agents promotes cleavage of the BT-R_1 ectodomain, resulting in formation of fragments that are similar to those observed during larval development. Partial purification of proteins from brush border membrane vesicles (BBMVs) by gel filtration chromatography hinders the cleavage of BT-R_1 in the presence of EDTA and EGTA, indicating that there is specific proteolytic activity associated with the BBMV. This specific proteolytic cleavage of BT-R_1 not only alters the integrity of BT-R_1 but it most likely is implicated in cell adhesion events during differentiation and development of *M. sexta* midgut epithelium. We propose a model for calcium-dependent protection of BT-R_1 as well as a cleavage pattern that may modulate the molecular interactions and adhesive properties of its ectodomain. Molecular characterization of such a protection mechanism should lead to a better understanding of how the function of specific cadherins is modulated during tissue differentiation and insect development.

Cadherins constitute a large family of transmembrane cell adhesion molecules that are central determinants in cell patterning and preserving tissue architecture in metazoan organisms (*1*−*5*). Functional characteristics of cadherins are attributed to their Ca^{2+}-dependent structural features (*6*−*9*). The ectodomain of cadherins contains Ca^{2+}-binding sites that stabilize its characteristic rodlike structure and preserve its adhesive function and molecular interactions (*10*−*15*). Defects in Ca^{2+} binding preclude cadherin adhesive function (*16*). Removal of Ca^{2+} or changes in the concentration of the ion affects the adhesive activity and induces conformational changes in the ectodomain rendering the cadherins vulnerable to proteases (*1*, *12*, *15*−*18*). Changes in the adhesive function of cadherins influence initiation and maintenance of intercellular junctions and overall cell function (*13*−*18*). However, such changes are important during development and morphogenesis because the adhesive functions of tissue-specific cadherins have crucial roles in cell differentiation, establishment of cell polarity, developmental patterning, and organ formation.

Previously, we characterized a new type of epithelial cadherin, BT-R_1 (M_r = 210 kDa), from the larval midgut of the tobacco hornworm *Manduca sexta* (ref *19*; GenBank AF310073). BT-R_1 is a target receptor for Cry1A toxins of the entomopathogenic soil bacterium *Bacillus thuringiensis* (*20*). The domain architecture and structural features of BT-R_1 (Figure 1) together with its tissue-specific expression in larvae point up the importance of the molecule in differentiation and development of midgut epithelium in *M. sexta* (*19*−*21*). In the present study, we show that larval development accompanies changes in the abundance of BT-R_1 concomitant to specific cleavage of the molecule in the different developmental stages (instars) of the larva. Because ectodomain integrity of cadherins depends on calcium, we were interested in knowing whether the stability of BT-R_1, likewise, is calcium dependent. The results of our investigations reveal that calcium, indeed, influences the structure of the BT-R_1 ectodomain and that, upon removal of calcium by chelating agents, the ectodomain is cleaved into two fragments (145 and 120 kDa), both of which bind to the Cry1Ab toxin of *B. thuringiensis*. However, BT-R_1 contained in BBMVs[1] became refractory to cleavage after purification of the BBMV by gel filtration, indicating that a specific protease(s), separable from BT-R_1, directly affects the integrity of the ectodomain. These results support our hypothesis that a

† This work was supported in part by grants from Pioneer Hi-Bred International, Inc., Johnston, IA, and the U.S. Agency for International Development (263-0240-G-00-6014-00).

* To whom correspondence should be addressed. Telephone: (972) 883-4226. Fax: (214) 648-1406. E-mail: lee.bulla@utdallas.edu.

‡ The University of Texas at Dallas.

§ These authors contributed equally to this work.

|| University of Wyoming.

[1] Abbreviations: BBMVs, brush border membrane vesicles; DTT, dithiothreitol; EDTA, ethylenediaminetetraacetic acid; EGTA, ethyleneglycol-bis(2-aminoethyl ether)-*N*,*N*,*N*,*N*′-tetraacetic acid; TLCK, tosyl lysyl chloromethyl ketone; TPCK, tosyl phenylalanyl chloromethyl ketone; PMSF, phenylmethanesulfonyl fluoride; PNSF, *p*-nitrobenzenesulfonyl fluoride; NBSF, *p*-nitrobenzenesulfonyl fluoride.

10.1021/bi026323k CCC: $22.00
Published on Web 10/25/2002

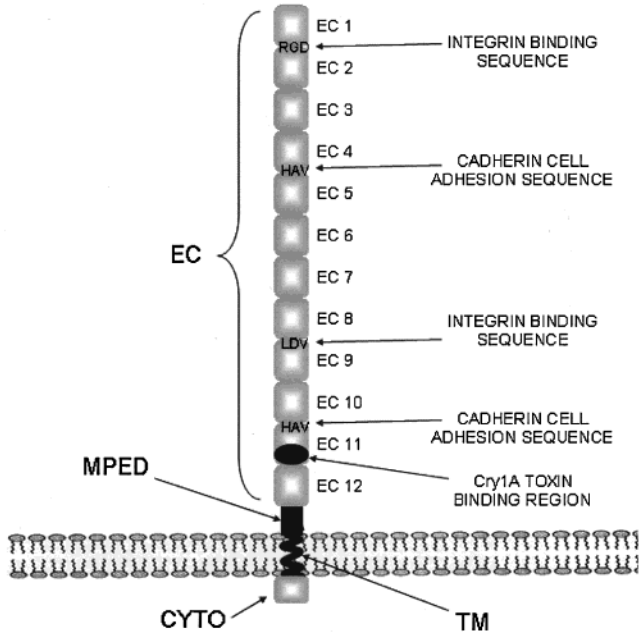

FIGURE 1: BT-R1 domain structure. The amino acid sequence of BT-R_1 was scanned using ProfileScan algorithm (http://hits.isb-sib.ch/cgi-bin/PFSCAN) to confirm the domain organization of the protein. BT-R_1 is composed of four domains: (i) EC (ectodomain), (ii) MPED (membrane-proximal extracellular domain), (iii) TM (transmembrane domain), and (iv) CYTO (cytoplasmic domain). The EC consists of 12 ectodomain modules (EC1-EC12). Putative calcium binding sequences are distributed throughout the ectodomain (*34*). The EC harbors a pair of putative cell-adhesion sequences, HAV (His-Ala-Val) and two putative integrin binding sequences RGD (Arg-Gly-Asp) and LDV (Leu-Asp-Val). The Cry1A toxin-binding region (dark elipse) folds into the EC11 close to the MPED.

critical decrease in Ca^{2+} concentration renders the BT-R_1 susceptible to protease(s), which specifically cleaves the ectodomain, thereby, altering its adhesive properties. A mechanism for the specific cleavage and modulation of molecular interactions of the BT-R_1 is proposed. We believe that cleavage of BT-R_1 and alteration of the adhesive properties of this specific cadherin may have functional significance in the differentiation and establishment of structural integrity of the midgut tissue during development of *M. sexta* larvae.

EXPERIMENTAL PROCEDURES

Preparation of M. sexta BBMVs and Detection of BT-R_1. Hornworm eggs and diet for larvae were obtained from Carolina Biological Supply Company. Eggs were placed on diet and incubated under constant light at room temperature in a 24 × 36 cm tray. Larvae were selectively harvested according to their stage of development (instar). Larvae with no signs of molting were designated as specific instars primarily according to their length: first instar, 5−8 mm; second instar, 9−18 mm; third instar, 19−30 mm; fourth instar, 31−45 mm; and fifth instar, 46−75 mm (*21*). Larval midguts (anterior, middle and posterior sections) were removed and BBMVs were prepared using the procedure described by Wolfersberger et al. (*23*). All preparations were stored at −70 °C in buffer A (10 mM Hepes, pH 9.5, 130 mM KCl, and 10% glycerol). In experiments involving divalent ion chelation, ethylenediaminetetraacetic acid (EDTA) and ethylene-glycol-bis(2-aminoethyl ether)-*N*,*N*,*N*′,*N*′-tetraacetic acid (EGTA) were used at a concentration of 10 mM. All results reported in this study using EDTA were similar with EGTA, and therefore, only the EDTA results are reported herein.

The BBMV proteins (50 μg/lane) were separated by SDS−PAGE in 8% gels and analyzed by radio-ligand blotting with [^{125}I]Cry1Ab, which provides a specific, high-affinity reagent for the detection of BT-R_1 (*19*, *20*). Iodination of Cry1Ab was accomplished as previously described (*24*, *25*). Autoradiography was performed at −70 °C, and radioligand bound proteins were detected using Kodak X-Omat AR film. The amount of radioligand-bound protein fragments was determined in excised protein bands using a gamma counter (Beckman Gamma 5500) as well as from radioligand blots using a Bio-Rad GS525 molecular imager system. Total counts in the sampling areas were recorded and analyzed with Molecular Analyst software. Identical areas from outside the samples were counted and subtracted as background. Protein loadings onto SDS−PAGE gels were adjusted based on protein concentrations that were determined with the BCA protein assay (Pierce) using bovine serum albumin (Sigma) as standard. The protein masses on all gels and blots were estimated according to SDS protein standards containing rabbit muscle myosin (205 kDa), *Escherichia coli* β-galactosidase (116 kDa), and rabbit muscle phosphorylase b (97 kDa) (Sigma, cat. no. M2789).

Cloning, Expression, and Purification of the BT-R_1 Ectodomain Fragment. A DNA fragment encoding 450 amino acid residues (amino acids 1078−1528) of the BT-R_1 ectodomain containing the Cry1Ab toxin binding region was cloned and expressed using plasmid vector pET30(b) in *E. coli* BL21(lambda DE3) (Novagen) cells. Most of the expressed fragment was sequestered in inclusion bodies within the bacterial cells. Inclusion bodies were collected as pellets by centrifugation at 16000*g* for 20 min at 4 °C. The pellets were washed three times in 50 mL of wash buffer (20 mM Tris-HCl, pH 7.5, 10 mM EDTA, 1% Triton X-100) and dissolved in 50 mL of solubilization buffer (50 mM CAPS, pH 11.0, 0.15% *N*-laurilsarcosine). After incubation in solubilization buffer for 15 min at room temperature, the protein was dialyzed against 20 mM Tris-HCl (pH 8.5) containing 0.1 mM DTT. Final dialysis was performed using the same buffer without DTT. The protein was purified using a nickel affinity column that was packed and activated as described by Novagen. After elution in buffer containing 1 M imidazole and 20 mM Tris-HCl (pH 8.0), the protein was dialyzed against 20 mM Tris-HCl (pH 8.0) and concentrated using a Centriplus YM-10 column (Millipore). The protein was further purified by FPLC using a Superdex 200 column (30 × 1 cm) (Amersham Biosciences) equilibrated with 10 mM Tris (pH 8.0).

Circular Dichroism (CD) Spectroscopy. CD spectra were obtained using a Jasco J-710 spectropolarimeter (Jasco Co., Tokyo, Japan). Spectra were recorded at 20 °C in a quartz cell with a path length of 1.0 mm by scanning in the 240−190 nm range at 0.1 nm intervals with a scan speed of 50 nm/min. Results were scaled to molecular ellipticity and presented as the averages of 10 accumulations and corrected for baseline that was obtained using the signal from the respective buffers. The concentration of the protein was 10 μM in 10 mM Tris-HCl buffer (pH 8.0) in the presence or absence of 5mM $CaCl_2$.

Protease Inhibitors. The effects of protease inhibitors and chemical modifying agents on EDTA- and EGTA-induced cleavage were tested in reaction mixtures containing 50 μg of BBMV proteins in buffer A at various pH values and temperatures. After 30 min of preincubation of BBMVs in the presence of chemical modifying agents, or specific protease inhibitors, the mixtures were further incubated with or without EDTA (10 mM) in buffer A (pH 9.5) at 4 °C for 24 h. The BBMVs were precipitated by centrifugation, resuspended in buffer A, and applied to gel. All chemicals were obtained from Sigma except sulfo-NHS-acetate, which was obtained from Pierce. The hydroxamic-acid-type metalloprotease inhibitor, KD-IX-73−4 (*26*), was provided by Dr. Kei Kishimoto of Boehringer Ingelheim. The following inhibitors and modifying agents were used at the specified concentrations: soybean trypsin inhibitor, chymostatin, and pepstatin A (10 μg/mL); phosphoramidon and 1,10-phenanthroline (50 μM); tosyl lysyl chloromethyl ketone (TLCK) and tosyl phenylalanyl chloromethyl ketone (TPCK) (0.1−1000 μM); *N*-ethylmalemide (0.5−5000 μM); iodoacetamide (5−50 mM); phenylmethanesulfonyl fluoride (PMSF) and *p*-nitrobenzenesulfonyl fluoride (PNSF) (0.1−2 mM).

Gel Filtration Chromatography of BBMVs. Partial solubilization of BBMVs was accomplished as previously described by Francis and Bulla (*27*) using a buffer containing 10 mM Hepes (pH 7.4), 130 mM KCl, 10% glycerol, 0.5% CHAPS, and 10 mM $CaCl_2$. Partially solubilized BBMVs were applied to a Superdex 200 column (30 × 1 cm) attached to an FPLC system (Amersham Biosciences) equilibrated with buffer A at 4 °C. Eluates were monitored at 280 nm and 1-mL fractions were collected for analysis. The proteins were examined before and after gel filtration by SDS−PAGE to confirm partial purification of the proteins.

RESULTS

Larval Development and Cleavage of BT-R_1. The expression pattern of cadherins during development is highly regulated and is essential to the morphogenesis of tissues and organs of vertebrates and invertebrates (*28*). To examine the expression of BT-R_1 during *M. sexta* larval development, BBMV proteins from different developmental stages (first through fifth instars) of the larva were analyzed by radioligand blotting (Figure 2). Results show that there is an overall increase in the abundance of the 210-kDa BT-R_1 throughout larval growth and development. As the larva progressed from first to fifth instar, smaller protein fragments, particularly a 145- and a 120-kDa fragment (Figure 2, arrows), were generated. Formation of the 145-kDa fragment was noticeable mainly in instars 3−5. The appearance of the 120-kDa fragment was prominent in the fifth instar larva. The dramatic increase in the abundance of BT-R_1 and the formation of the 145- and 120-kDa fragments coincided with the period during which the larva exhibited phenomenal growth, especially in the fifth instar. The build-up of BT-R_1 in the midgut epithelium may reflect a differentiation process that establishes the specialized structure and function of epithelial cells in the midgut tissue. The smaller molecular-weight bands observed in Figure 2 may be the result of nonspecific binding of the Cry1Ab toxin to BBMV proteins as has been demonstrated by Daniel et al. (*29*). Alternatively, the smaller bands may represent products of further cleavage of the BT-R_1 in the midgut.

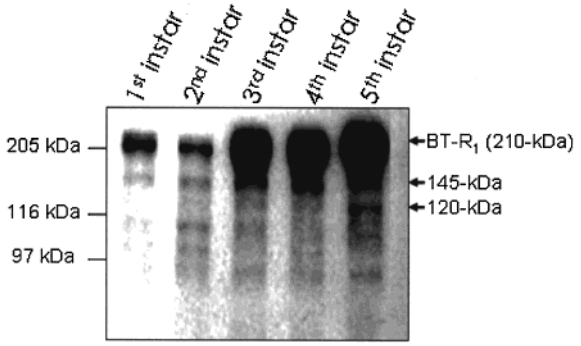

FIGURE 2: BT-R1 expression in *M. sexta* larval development. Larvae with no signs of molting were selected according to their developmental size. Midguts (anterior, middle, and posterior sections) were removed and BBMV proteins (50 μg) for all five instars were analyzed by radio-ligand blotting using [^{125}I]Cry1Ab, which binds specifically and with high-affinity to BT-R_1 (*33*, *34*). The larval developmental stages from which BBMV proteins were isolated are indicated as instars for each lane. Protein loadings were adjusted based on protein concentrations that were determined with the BCA protein assay (Pierce) using bovine serum albumin (Sigma) as standard. The protein masses in this figure as well as all other figures below were estimated according to SDS protein standards containing rabbit muscle myosin (205 kDa), *E. coli* β-galactosidase (116 kDa), and rabbit muscle phosphorylase b (97 kDa) (Sigma, cat. no. M2789).

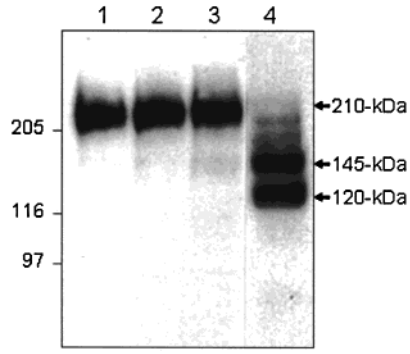

FIGURE 3: Ligand blot analysis of BT-R1 in the presence of metal ions and EDTA. BBMVs from fifth-instar *M. sexta* larvae were incubated for 24 h at 4 °C in 10 mM Hepes, 130 mM KCl, pH 9.5, containing 5 mM $CaCl_2$ (lane 1), 5 mM $SrCl_2$ (lane 2), 5 mM $MgCl_2$ (lane 3), and 10 mM EDTA alone (lane 4). Proteins (50 μg) were separated by SDS−PAGE and [^{125}I]Cry1Ab toxin binding was examined on a nylon membrane by ligand blotting.

Effects of Divalent Metal Ions on BT-R_1. Because the integrity of cadherins depends on calcium ions which bind to and stabilize the ectodomain, the effects of different metal ions and chelating agents on the integrity of BT-R_1 was examined by adding $CaCl_2$, $SrCl_2$, $MgCl_2$, to the BBMV-toxin incubation mixture. The physiological concentration of calcium in the *M. sexta* larval midgut is 1−10 mM (*30*), a range sufficient to protect cadherins from proteolysis (*31*, *32*). As can be seen in Figure 3, binding of [^{125}I]Cry1Ab to BT-R_1 was not altered by any of the three metal ions as observed in Western blot experiments (Figure 3, lanes 1−3). However, upon addition of EDTA, binding of toxin to full-length BT-R_1 was reduced markedly because of its cleavage to the 145- and 120-kDa fragments which appeared to retain high toxin-binding affinity (Figure 3, lane 4, arrows). Results obtained using EDTA were similar with EGTA, and therefore, only the EDTA results are shown in this and the following figures. Similar observations have been reported by Martinez-Ramirez et al. (*33*).

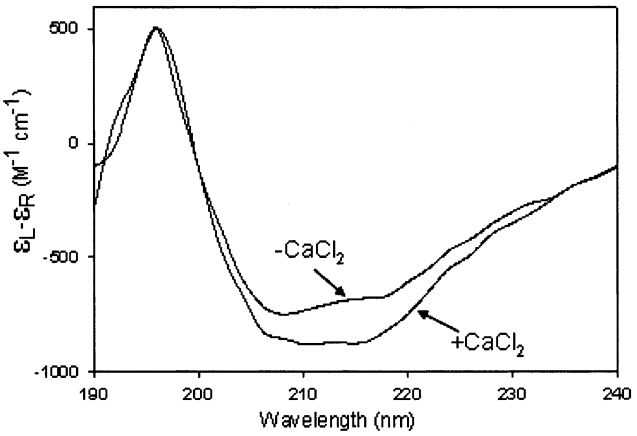

FIGURE 4: CD spectra of BT-R1 ectodomain fragment. The spectra of the recombinant BT-R_1 fragment were recorded using a 1-mm quartz cell at a protein concentration of 10 μM in a buffer containing 10 mM Tris·HCl, pH 8, with calcium (5 mM $CaCl_2$) and without calcium at 20 °C. Results from 10 measurements were averaged and scaled to molecular elipticity.

Influence of Calcium on the BT-R_1 Ectodomain. The conformation, structural integrity, and adhesive function of cadherin ectodomain depend largely on extracellular calcium influxes (*15*, *34*). To determine the extent of the influence of calcium on the conformation of BT-R_1, the effects of Ca^{2+} ions on the CD spectrum of a segment encompassing EC10-EC12 of the BT-R_1 ectodomain to which Cry1Ab toxin binds was examined (see Figure 4). The spectrum of the fragment (Figure 2) was similar to the spectrum of mammalian E-cadherin ectodomain whose main secondary structure consists of β -sheets (*16*, *35*, *36*). The shape of the spectrum for the BT-R_1 fragment (Figure 4) indicates the presence of a large fraction of β -structure in the molecule. The β-structure conformation remained intact in either the absence or the presence of Ca^{2+}. However, a significant decrease in the molar elipticity at 215 nm was observed in the presence of $CaCl_2$ (Figure 4). This phenomenon suggests that the BT-R_1 ectodomain undergoes structural changes upon binding of Ca^{2+}. In other words, the conformational change of the EC10-EC12 fragment may reflect a Ca^{2+}-dependent structural transformation of the ectodomain. Both the nature and magnitude of the observed decrease are similar to those described for other cadherins (*13*).

Calcium-Dependent Sequential Cleavage of BT-R_1. Removal of calcium affects the conformation and, subsequently, the integrity of cadherin ectodomain. To gain insight into the influence of calcium on the integrity of BT-R_1, a time-course radio-ligand blot analysis was performed. (Figure 5). The analysis revealed that there is an increase in the formation of the 145- and 120-kDa fragments in the presence

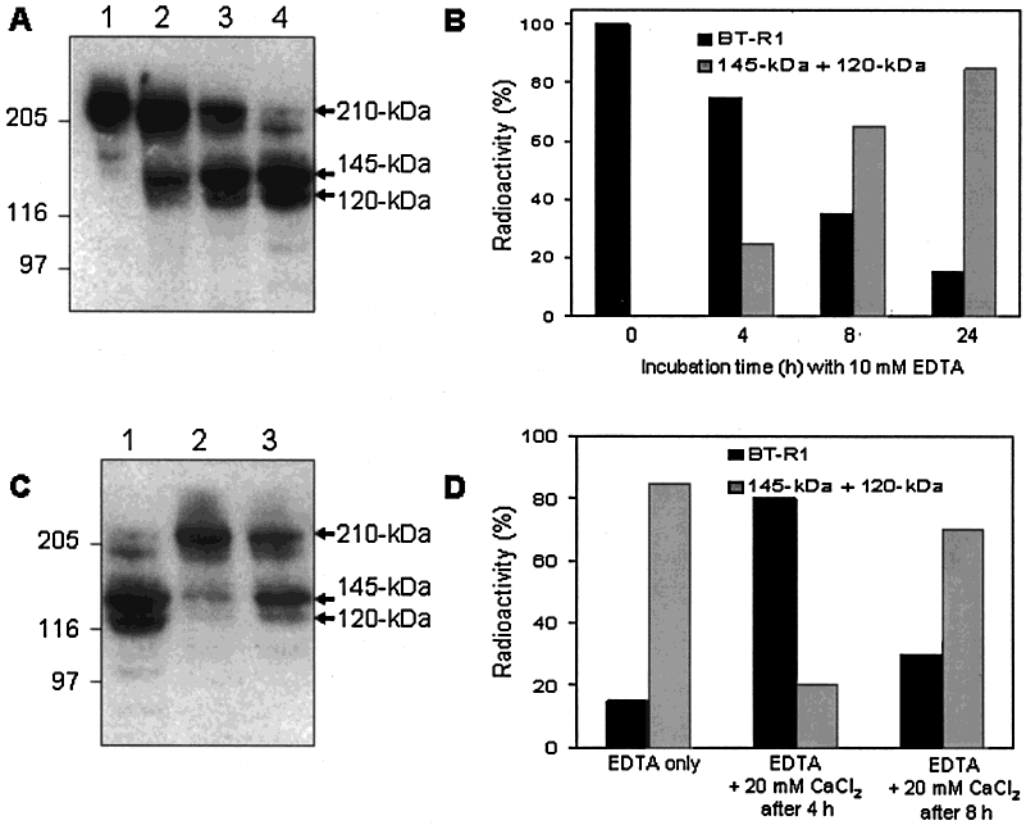

FIGURE 5: Time-course ligand blot analysis of BT-R_1 in the presence of EDTA and $CaCl_2$. (A) BBMVs from fifth-instar *M. sexta* larvae were incubated for 24 h at 4 °C in 10 mM Hepes, 130 mM KCl, pH 9.5, containing 10 mM EDTA, and [^{125}I]Cry1Ab toxin binding to the 210-kDa cadherin BT-R_1 and the 145- and 120-kDa cleavage products was examined. Lane 1 contains BBMV proteins incubated for 24 h at 4 °C in buffer without EDTA. Lanes 2, 3, and 4 are ligand blots of BBMV proteins incubated with EDTA for 4, 8, and 24 h, respectively. (B) Relative levels of [^{125}I]CryAb toxin bound to BT-R_1 and to the combined 145- and 120-kDa fragments at 0, 4, 8, and 24 h of incubation with EDTA. (C) Effect of $CaCl_2$ on the formation of the 145- and 120-kDa fragments on BBMVs. Lane 1, BBMV proteins incubated for 24 h in buffer containing 10 mM EDTA only. Lane 2, BBMV proteins incubated for 4 h in buffer containing 10 mM EDTA and for an additional 20 h after 25 mM $CaCl_2$ was added. Lane 3, BBMV proteins incubated for 8 h in buffer containing 10 mM EDTA and incubated for an additional 16 h after 25 mM $CaCl_2$ was added. (D) Effect of $CaCl_2$ on the levels of [^{125}I]CryAb toxin binding to BT-R_1 and the 145- and 120-kDa fragments combined. Forty micrograms of BBMV protein was applied to each lane for analysis.

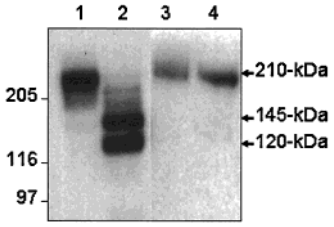

FIGURE 6: Effect of gel chromatography on the cleavage of BT-R1. Partially solubilized BBMVs (see Experimental Procedures) was filtered through a Superdex 200 column attached to an FPLC system. Eluates were monitored at 280 nm and 1-mL fractions were collected for analysis. General endoproteolytic activity was unaltered after the gel filtration as previously reported (*27*). The proteins were examined before and after gel filtration by SDS−PAGE to confirm partial purification of the proteins. The BBMV proteins (50 μg) were analyzed by ligand blotting with [^{125}I]Cry1Ab toxin. Lanes 1 and 2, BBMV proteins incubated in buffer without EDTA and with 10 mM EDTA, respectively. Lanes 3 and 4, BBMV proteins filtered through a Superdex 200 column incubated in buffer without EDTA and with 10 mM EDTA, respectively.

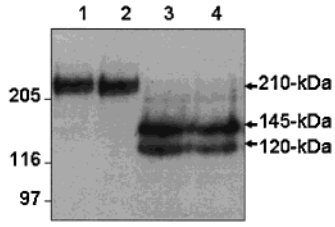

FIGURE 7: Radioligand blot analysis of BBMVs preincubated with unlabeled Cry1Ab toxin in the absence and presence of EDTA. BBMVs were preincubated with or without 100 nM Cry1Ab toxin in the absence or presence of EDTA for 24 h at 4 °C in 10 mM Hepes, 130 mM KCl, pH 9.5. Lane 1, BBMV proteins in buffer without EDTA; lane 2, Cry1Ab-treated BBMVs in buffer without EDTA; lane 3, BBMV proteins in buffer with 10 mM EDTA; lane 4, Cry1Ab-treated BBMVs in buffer with 10 mM EDTA. The intensity of labeled bands on the blots with [^{125}I]Cry1Ab is comparable in each lane because the labeled toxin efficiently removes unlabeled toxin from the same binding site on BT-R_1 (*20*).

of EDTA or EGTA, which corresponds to a decrease in the amount of the 210-kDa BT-R_1 molecule (Figure 5A, lanes 2−4). The amount of the 145- and 120-kDa fragments after incubation in EDTA or EGTA varied considerably with time (up to 24 h) although the total amount of BT-R_1 and the two fragments remained virtually the same throughout the time course (Figure 5B). Treatment of BBMVs with 10 mM EDTA or EGTA for 24 h resulted in the disappearance of ~85% of the 210-kDa BT-R_1 band (Figure 5A, lane 4) and led to the accumulation of the 145- and 120-kDa fragments (Figure 5B). Further incubation up to 48 h (data not shown) resulted in complete disappearance of the 210-kDa band, and no other protein fragments other than the 145- and 120-kDa protein bands were produced. These results indicate that incubation of BBMVs in either of the chelating agents apparently did not expose other proteins that are inaccessible on the membrane and that the 145- and 120-kDa fragments are products of sequential cleavage of BT-R_1. Addition of Ca^{2+} to the incubation mixture containing EDTA or EGTA at 4 and 8 h blocked the accumulation of the 145- and 120-kDa fragments (Figure 5C, lanes 2 and 3, respectively) and prevented any further fragment accumulation in the reactions. Figure 5D shows the extent of fragment accumulation at 24 h in the reactions to which $CaCl_2$ was added at 4 and 8 h. Efficient production of 145- and 120-kDa fragments occurred at pH 8−10 which corresponds to the physiological pH in the midgut of *M. sexta* larvae and only minimal production of the fragments was observed at pH 7 and lower (data not shown).

Involvement of BBMVs in the Specific Cleavage of BT-R_1. The cleavage of BT-R_1 does not appear to be the result of proteolytic activity associated with BT-R_1 itself because partial purification of BT-R_1 by gel filtration excludes any such activity (Figure 6). Previously, we reported that partial solubilization of BBMVs using 0.5% CHAPS followed by gel filtration does not affect the general endoproteolytic activity in the eluates (*27*). As can be seen in Figure 6 (lanes 3 and 4), incubation of gel filtration-purified BT-R_1 with EDTA or EGTA did not bring about formation of the 145- and 120-kDa fragments, indicating that there is a protease(s) residing on the BBMV that specifically cleaves BT-R_1. Moreover, there was no apparent degradation of the total BBMV proteins in the presence of EDTA or EGTA (data not known). Thus, chelation of divalent metal ions appears to increase the susceptibility of BT-R_1 to specific cleavage, either by exposing a segment of the protein that is normally resistant to proteolysis or by activating a specific protease on the BBMV. Interestingly, a variety of chemical modifying agents and protease inhibitors did not result in blocking the proteolysis of BT-R_1. Treatment of BBMVs with NBSF, TLCK, TPCK, *N*-ethylmalamide, and sulfo-NHS-acetate did not affect the cleavage of BT-R_1 (data not shown). Soybean trypsin inhibitor, chymostatin, pepstatin A, iodoacetamide, PNSF, PMSF, as well as metalloprotease inhibitors 1,10-phenanthroline, phosphoramidon, and KD-IX-73−4, which is an inhibitor for selectin cleavage, also did not affect the cleavage of BT-R_1 individually or in combination under a variety of experimental conditions. In all cases, EDTA and EGTA treatment resulted in the formation of the 145- and 120-kDa Cry1Ab toxin binding fragments (data not shown).

Specific Cleavage of BT-R_1 and Cry1Ab Toxin Binding. To determine whether Cry1Ab binding to BBMVs affects the proteolytic cleavage of BT-R_1 in the presence of EDTA or EGTA, BBMVs were preincubated with and without unlabeled Cry1Ab toxin (Figure 7). Preincubation with unlabeled Cry1Ab did not affect binding of the labeled toxin to the BT-R_1 in the absence of the two chelating agents (Figure 7, lane 2), nor did toxin binding inhibit the formation of the 145- and 120-kDa fragments in the presence of them (Figure 7, lane 4). There was no noticeable reduction in [^{125}I]-Cry1Ab toxin binding to the protein bands on the blots, indicating that preincubation of BBMVs with unlabeled Cry1Ab toxin did not interfere with the specific cleavage sites on the BT-R_1 receptor.

The Pattern of Cleavage of BT-R_1 on BBMVs. To determine the pattern of cleavage of BT-R_1 in the presence of EDTA and EGTA, we examined [^{125}I]Cry1Ab toxin binding to both soluble and membrane-bound fractions after treatment of BBMVs with the two chelating agents for a 24-h period (Figure 8). Membrane-bound and soluble proteins were separated by centrifugation and blotted on PVDF membrane. Radiolabeled toxin bound to the 145- and 120-kDa protein fragments in the precipitated fraction (Figure 8, lane 3) but not in the soluble fraction (Figure 8, lane 2). Addition of DTT (final concentration of 5 mM) to the incubation mixture did not affect the cleavage of BT-R_1 (Figure 8, lane 4) or the retention of the 145- and 120-kDa

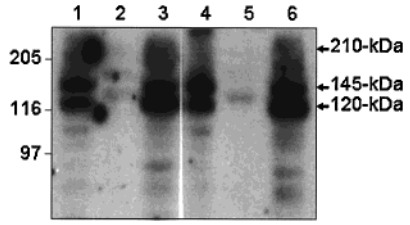

FIGURE 8: Ligand blot analysis of soluble and membrane-bound fractions of EDTA-treated BBMV proteins. BBMVs were incubated for 24 h at 4 °C in the presence of 10 mM EDTA (pH 9.5). The incubation mixture was centrifuged for 10 min at 8000*g* in a microcentrifuge tube. [^{125}I]Cry1Ab toxin-binding proteins in the pellet (membrane-bound) and supernatant (soluble) were examined on blots. Lane 1, total incubation mixture before centrifugation of BBMVs; lane 2, soluble fraction of BBMVs incubated with EDTA; lane 3, membrane bound fraction of BBMVs incubated with EDTA; lanes 4−6, same as lanes 1−3 except 5 mM DTT was added to the incubation mixture.

toxin-binding fragments on the membrane-bound fraction (Figure 8, lane 6). Obviously, a significantly large portion of BT-R_1 ectodomain, containing the toxin binding region, remains attached to the membrane after cleavage of BT-R_1, and this cleavage is not dependent on the oxidized/reduced state of the molecule.

DISCUSSION

Both in vivo and in vitro studies have demonstrated that calcium ions affect the structural stability and specific regions of cadherins that are essential to adhesion function and various interactions on the cell surface (*6*−*9*, *37*−*43*). Adhesion and interactions of cells with their neighboring cells provide not only mechanical support but the necessary signals for regulation of cellular processes and their morphological states as well (*44*, *45*). Such interactions are crucial in maintaining normal epithelial organization and differentiation of cells in epithelial tissues. Furthermore, oncogenic properties of various signaling pathways are linked to cell adhesion events involving cadherins. Calcium influx or depletion of the ions triggers specific proteolysis of cadherins resulting in rapid destruction of intercellular adhesion junctions, which apparently are important in the proliferation and migration of epithelial cells during development and morphogenesis and in regeneration of mucosal tissues (*18*, *34*, *46*, *47*). Cleavage of extracellular domains of cadherins is mechanistically important in modulating the function of cadherins and is required for the assembly and disassembly of cell junctions and dissociation of cells from tissues in response to change in calcium concentrations (*18*, *48*−*51*).

M. sexta BT-R_1 (M_r = 210 kDa) (GenBank AF319973) represents a new type of cadherin, which is composed of an ectodomain (EC) with 12 EC modules, a membrane-proximal extracellular domain (MPED), a transmembrane domain (TM), and a cytoplasmic domain (CYTO) (Figure 1). The ectodomain contains putative calcium-binding sequences distributed throughout the ectodomain (*20*). The ectodomain harbors two cell-adhesion sequences, HAV (His-Ala-Val), which is important for cadherin function (*52*). The ectodomain also contains integrin binding sequences RGD (Arg-Gly-Asp) and LDV (Leu-Asp-Val) that usually are found in fibronectin (*53*−*60*). BT-R_1 is involved in the toxic action of Cry1A toxins produced by the entomopathogenic bacterium *B. thuringiensis* (*20*). Our previous findings showed that

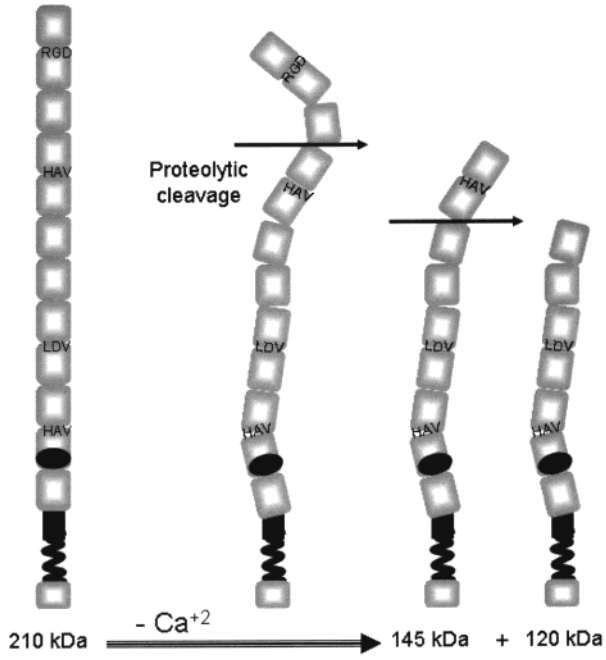

FIGURE 9: Proposed model for cleavage of BT-R_1. Calcium ions stabilize the structural conformation of BT-R_1 on membrane. Removal of calcium leads to destabilization of the BT-R_1 structure, causing susceptibility to proteolytic attack. Sequential proteolytic cleavage involves two sites within a region between EC3 and EC6 of BT-R_1 and results in the formation of 145- and 120-kDa ectodomain fragments retained on the membrane.

Cry1Aa, Cry1Ab, and Cry1Ac toxins bind to a specific toxin binding region (TBR) on BT-R_1 located on EC11 (*20*). Now, we report that chelation of calcium by EDTA or EGTA leads to cleavage of BT-R_1 and causes formation of two fragments, 145- and 120-kDa, both of which bind to Cry1Ab toxin. This finding indicates that the TBR, which folds into EC11, is represented in both of the fragments generated by treatment with either of the two chelating agents. Preincubation of BBMVs with Cry1Ab toxin prior to incubation with EDTA or EGTA did not inhibit the cleavage of BT-R_1, indicating that the toxin binding and cleavage sites are mutually exclusive. The 145- and 120-kDa fragments were generated sequentially (Figure 5, panels A and B), and both fragments were retained in membrane-bound fractions after EDTA or EGTA treatment of BBMVs. Moreover, the addition of calcium stopped the sequential formation of the 145- and 120-kDa protein bands, and these fragments were not further cleaved in the presence of EDTA or EGTA. Collectively, the data support the supposition that the cleavage pattern of BT-R_1, as well as the sites of cleavage, is specific.

The sequential cleavage of BT-R_1 involves at least two sites (see model in Figure 9). According to this model, cleavage of BT-R_1 correlates with calcium removal and takes place at a region between EC3 and EC6 where BT-R_1 displays an E-cadherin folding motif and contains one of the potential cadherin cell adhesion recognition sequences (HAV). Presumably, removal of calcium alters the structural stability of BT-R_1 and exposes the EC3-EC6 region to a protease(s), resulting in a specific cleavage pattern of BT-R_1. Cleavage of BT-R_1 in this region may have functional significance during larval development in that the molecule becomes detached from the N-terminal portion containing the integrin-binding sequence RGD as well as one of the

potential cadherin-binding sequences (HAV), while retaining the other potential binding sequences for integrin (LDV) and cadherin (HAV). Indeed, the scheme depicted in Figure 9 could explain how specific cleavage modulates the adhesive properties of BT-R_1 in vivo, depending on calcium ion concentration.

The proteolytic activity related to the cleavage of BT-R_1 does not reside in BT-R_1 itself because this activity can be separated from BT-R_1 when BBMVs are solubilized and passed through a gel filtration column (Figure 6). The protease(s) on BBMVs appears to exhibit specificity for the cleavage of BT-R_1. This type of behavior is characteristic of the activity of certain membrane enzymes such as secretases and sheddases, many of which are Zn^{2+}-dependent membrane metalloproteinases (*26*, *45*, *61*−*65*). Although these proteases mediate the cleavage of various membrane-anchored proteins, including cadherins, specific proteases have not been identified yet. The cleavage of BT-R_1 upon removal of calcium is not prevented by metalloprotease inhibitors phosphoramidon, KD-IX-73-4, and 1,10-phenanthroline (data not shown). Perhaps, the enzymes that act on BT-R_1 have a mode of action different from the established families of metalloproteinases because the pH of the *M. sexta* midgut is high (pH 10.5). Under such an alkaline condition, lysine or tyrosine groups may exist in the active site of a proteinase because these side chains generally have p*K* values of ∼10 and they may be better able to function in acid−base catalysis than the imidazole group of histidine, the thiol group of cysteine or the carboxylate groups of aspartate and glutamate. But, addition of sulfo-NHS-acetate, which modifies lysine residues, had no effect on proteolysis at a concentration of 5 mg/mL. At a concentration of 10 mg/mL, proteolysis increased. Furthermore, addition of NBSF, a tyrosine modifying reagent, likewise had no effect (data not shown).

Specific proteolytic cleavage of cadherin ectodomains is an important aspect of cell regulation and cell interactions (*61*, *66*). Developmental and tissue-specific expression of BT-R_1 in the midgut of *M. sexta* larvae supports our hypothesis that the cleavage of the BT-R_1 ectodomain is important to specific cell interactions in the midgut epithelium. The midgut consists of highly structured epithelial cells that are organized in a characteristic pattern (*67*). During larval development (including growth and larval-larval molts), the organization of *M. sexta* midgut cells undergoes dramatic arrangements to support cell proliferation as well as structural and functional integrity of the tissue indicating involvement of dynamic cell−cell adhesion events in this insect (*68*, *69*) as is true for all metazoan tissues (*66*, *70*, *71*). Some of the activities associated with cadherins involve not only cell−cell adhesion events but also activation of specific intracellular signaling pathways as well. Thus, increased proteolysis of cadherins, which has been implicated in various morphogenetic events, affects both cell−cell contact and cell−cell communication (*18*, *34*, *44*−*51*). The increase in BT-R_1 proteolysis that occurs, especially in the fifth instar, precedes the destruction of larval midgut epithelium prior to replacement by pupal epithelium (*72*, *73*), reflecting turnover of this particular cadherin at the end of larval development. Further studies are necessary to elucidate the functional significance of Ca^{2+}-dependent proteolysis of BT-R_1 in the larval midgut epithelium of *M. sexta*. Certainly, isolation and characterization of the proteolytic activity related to the cleavage of the cadherin receptor BT-R_1, as well as determination of the cleavage sites on the molecule, are important aspects for future investigations. Determining the specific cleavage pattern, modulation of interactions, and the clustering of cadherins on cell surfaces may provide insight into how specific cell adhesion events participate in epithelial cell proliferation, differentiation, cell migration, tissue structuring, wound repair, and programmed cell death, not to mention a variety of pathophysiological conditions, including cancer.

ACKNOWLEDGMENT

We are grateful to Donald M. Gray (University of Texas at Dallas) for his advice in the circular dichroism spectral analyses.

REFERENCES

1. Takeichi, M. (1991) *Science 251*, 1451−1455.
2. Takeichi, M. (1995) C*urr. Opin. Cell Biol. 7*, 619−627.
3. Yap, A. S., Brieher, W. M., and Gumbiner, B. M. (1997) *Annu. Rev. Cell. Dev. Biol. 13*, 119−146.
4. Le, T., Yap, A., and Stow, J. (1999) *J. Cell Biol. 146*, 219−232.
5. Nollet, F., Kools, P., and van Roy, F. (2000) *J. Mol. Biol. 299*, 551−572.
6. Kartenbeck, J., Schmid, E., Franke, W. W., and Geiger, B. (1982) *EMBO J. 1*, 725−732.
7. Mattey, D. L., and Garrod, D. R. (1986) *J. Cell Sci. 85*, 113−124.
8. Volberg, T., Geiger, B., Kartenbeck, J., and Franke, W. W. (1986) *J. Cell Biol. 102*, 1832−1842.
9. Green, K. J., Geiger, B., Jones, J. C. R., Talian, J. C., and Goldman, R. D. (1987) *J. Cell Biol. 104*, 1389−1402.
10. Overduin, M., Harvey, T. S., Bagby, S., Tong, K., Yau, P., Takeichi, M., and Ikura, M. (1995) *Science 267*, 386−389.
11. Shapiro, L., Fannon, A. M., Kwong, P. D., Thompson, A., Lehmann, M. S., Grubel, G., Legrand, J. F., Als-Nielson, J., Colman, D. R., and Hendrickson, W. A. (1995) *Nature 374*, 327−337.
12. Nagar, B., Overduin, M., Ikura, M., and Rini, J. M. (1996) *Nature 380*, 360−364.
13. Ozawa, M., Engel, J., and Kemler, R. (1990) *Cell 63*, 1033−1038.
14. Tamura, K., Shan, W. S., Hendrickson, W. A., Colman, D. R., and Shapiro, L. (1998) *Neuron 20*, 1153−1163.
15. Boggon, T. J., Murray, J., Chappuis-Flament, S., Wong, E., Gumbiner, B. M., and Shapiro, L. (2002) *Science 296*, 1308−1313.
16. Pertz, O., Bozic, D., Koch, A. W., Fauser, C., Brancaccio, A., and Engel, J. (1999) *EMBO J. 18*, 1738−1747.
17. Thomson, R. B., Igarashi, P., Biemesderfer, D., Kim, R., Abu-Alfa, A., Soleimani, M., and Aronson, P. S. (1995) *J. Biol. Chem. 270*, 17594−17601.
18. Troyanovsky, R. B., Klingelhofer, J., and Troyanovsky, S. (1999) *Cell Sci. 122*, 4379−4387.
19. Vadlamudi, R. K., Weber, E., Ji, I., Ji, T. H., and Bulla, L. A., Jr. (1995) *J. Biol. Chem. 270*, 5490−5494.
20. Dorsch, J. A., Candas, M., Griko, N. B., Maaty, W. S. A., Midboe, E. G., Vadlamudi, R., and Bulla, L. A., Jr. (2002) *Insect Biochem. Mol. Biol. 32*, 1025−1036.
21. Midboe, E. G., Candas, M., Dorsch, J. A., and Bulla, L. A., Jr. (2001) *SAAS Bulletin Biotech. Biochem. 14*, 73−80.
22. Eaton, J. L. (1988) *Lepidopteran Anatomy*, Vol. 1, Wiley-Interscience, New York.
23. Wolfersberger, M., Lüthy, P., Maurer, A., Parenti, P., Sacchi, F. V., Giordana, B., and Hanozet, G. M. (1987) *Comp. Biochem. Physiol. 86A*, 301−308.
24. Vadlamudi, R. K., Ji, T. H., and Bulla, L. A., Jr. (1993) *J. Biol. Chem. 268*, 12334−12340.
25. Keeton, T. P., and Bulla, L. A., Jr. (1997) *Appl. Environ. Microbiol. 63*, 3419−3425.
26. Feehan, C., Darlak, K., Kahn, J., Walcheck, B., Spatola, A. F., and Kishimoto, T. K. (1996) *J. Biol. Chem. 271*, 7019−7024.

27. Francis, B. R., and Bulla, L. A., Jr. (1997) *Insect Biochem. Mol. Biol. 27*, 541−550.
28. Gumbiner, B. M. (2000) *J. Cell Biol. 148*, 399−404.
29. Daniel, A., Sangadala, S., Dean, D. H., and Adang, M. J. (2002) *Appl. Environ. Microbiol. 68*, 2106−2112.
30. Dow, J. A., Gupta, B. L., Hall, T. A., and Harvey, W. R. (1984) *J. Membr. Biol.* 77, 223−241.
31. Hyafil, F., Babinet, C., and Jacob, F. (1981) *Cell 26*, 447−454.
32. Jensen, P. J., and Wheelock, M. J. (1992) *Exp. Cell Res. 202*, 190−198.
33. Martinez-Ramirez, A. C., Gonzalez-Nebauer, S., Escriche, B., and Real, M. D. (1994) *Biochem. Biophys. Res. Commun. 201*, 782−787.
34. Ito, K., Okamoto, I., Araki, N., Kawano, Y., Nakao, M., Fujiyama, S., Tomita, K., Mimori, T., and Saya, H. (1999) *Oncogene 18*, 7080−7090.
35. Pokutta, S., Herrenknecht, K., Kemler, R., and Engel, J. (1994) *Eur. J. Biochem. 223*, 1019−1026.
36. Koch, A. W., Bozic, D., Pertz, O., and Engel. J. (1999) *Curr. Opin. Struct. Biol. 9*, 275−281.
37. Gumbiner, B. M. (1996) *Cell 84*, 345−357.
38. Kinch, M. S., Petch, L., Zhong, C., and Burridge, K. (1997) *Cell. Adhes. Commun. 4*, 425−437.
39. Braga, V. M. (1999*) Mol. Pathol. 52*, 197−202.
40. Pece, S., and Gutkind, J. S. (1999) *J. Biol. Chem. 275*, 41227−41233.
41. Meredith, J. E., and Schwartz, M. A. (1997) *Trends Cell. Biol. 7*, 146−150.
42. Giancotti, F. G., and Ruoslahti, E. (1999) *Science 285*, 1028−1032.
43. Aplin, A. E., Short, S. M., and Juliano, R. L. (1999) *J. Biol. Chem. 274*, 31223−31228.
44. Werb, Z. (1997) *Cell 91*, 439−442.
45. Streuli, C. (1999) *Curr. Opin. Cell. Biol. 11*, 634−640.
46. Potter, S. W., Gaza, G., and Morris, J. E. (1996) *J. Cell. Physiol. 169*, 1−14.
47. Moriyama, N., Ishihara, S., Hirose, M., Watanabe, S., Sato, N., and Kinoshita, Y. (2001) *J. Lab. Clin. Med. 138*, 236−242.
48. Ozawa, M., and Kemler, R. (1992) *J. Cell Biol. 116*, 989−996.
49. Aberle, H., Schwartz, H., and Kemler, R. (1996*) J. Cell Biochem. 61*, 514−523.
50. Klingelhofer, J., Troyanovsky, R. B., Laur, O. Y., and Troyanovsky, S. (2000) *J. Cell Sci. 113*, 2829−2836.
51. Steinhusen, U., Weiske, J., Badock, V., Tauber, R., Bommert, K., and Huber, O. (2001) *J. Biol. Chem. 276*, 4972−4908.
52. Blaschuk, O. W., Sullivan, R., David, S., and Pouliot, Y. (1990) *Dev. Biol. 139*, 227−229.
53. Yamada, K. M., and Kennedy, D. W. (1984) *J. Cell. Biol. 99*, 29−36.
54. Pierschbacher, M. D., and Ruoslahti, E. (1987) *J. Biol. Chem. 262*, 17294−17298.
55. D'Souza, S. E., Ginsberg, M. H., Burke, T. A., Lam, S. C., and Plow, E. F. (1988) *Science 242*, 91−93.
56. Ruoslahti, E. (1996) *Annu. Rev. Cell. Dev. Biol. 12*, 697−715.
57. Wayner, E. A., Garcia-Pardo, A., Humphries, M. J., McDonald, J. A., and Carter, W. G. (1989) *J. Cell Biol. 109*, 1321−1330.
58. Mould, A. P., Wheldon, L. A., Komoriya, A., Wayner, E. A., Yamada, K. M., and Humphries, M. J. (1990) *J. Biol. Chem. 265*, 4020−4024.
59. Komoriya, A., Green, L. J., Mervic, M., Yamada, S. S., Yamada, K. M., and Humphries, M. J. (1991) *J. Biol. Chem. 266*, 15075−15079.
60. Tselepis, V. H., Green, L. J., and Humphries, M. J. (1997) *J. Biol. Chem. 272*, 21341−21348.
61. Hooper, N. M., Karren, E. H., and Turner, A. J. (1997) *Biochem. J. 321*, 265−279.
62. Werb, Z., and Yan, Y. (1998) *Science 282*, 1279−1280.
63. Paradies, N. E., and Grunwald, G. B. (1993) *J. Neurosci. 36*, 33−45.
64. Arribas, J., Coodly, L., Vollmer, P., Kishimoto, T. K., Rose-John, S., and Massague, J. (1996) *J. Biol. Chem. 271*, 11376−11382.
65. Nagase, H. (1996) in *Matrix Metalloproteinases in Zinc Metalloproteases in Health and Disease* (Hooper, N. M., Ed.) Taylor and Francis, London.
66. Peschon, J. J., Slack, J. L., Reddy, P., Stocking, K. L., Sunnarborg, S. W., Lee, D. C., Russell, W. E., Castner, B. J., Johnson, R. S., Fitzner, J. N., Boyce, R. W., Nelson, N., Kozlosky, C. J., Wolfson, M. F., Rauch, C. T., Cerretti, D. P., Paxton, R. J., March, C. J., and Black, R. A. (1998) *Science 282*, 1281−1284.
67. Baldwin, K. M., Hakim, R. S., Loeb, M. J., and Sadrud-din, S. Y. (1996) Midgut Development. In *The Insect Midgut* (Lehane, M. J., and Billingsly, P. F., Eds.) Chapman & Hall, London.
68. Hakim, R. S., Hakim, F. T., and Loeb, M. J. (1997) Growth of *Manduca sexta* midgut epithelial cells in the establishment of a primary culture. In *Invertebrate Cell Culture* (Maramorosch, K., and Mitsuhashi, J., Eds.) Science Publishers Inc., New Hampshire, pp 19−24.
69. Baldwin, K. M., and Hakim, R. S.(1991) *Tissue Cell 23*, 411−422.
70. McNeill, H. (2000) *Nat. Rev. Genet. 1*, 100−108.
71. Nathke, I. S., Hinck, L., Swedlow, J. R., Papkoff, J., and Nelson, W. J. (1994) *J. Cell. Biol. 125*, 1341−1352.
72. Russell, V. W., and Dunn, P. E. (1991) *Arch. Insect Biochem. Physiol. 17*, 67−80.
73. Uwo, M. F., Ui-Tei, K., Park, P., and Takeda, M. (2002) *Cell Tissue Res. 308*, 319−331.

BI026323K